ORIC: Benchmarking Object Recognition in Incongruous Context for Large Vision-Language Models

Zhaoyang Li[1*] Zhan Ling[1*] Yuchen Zhou[1] Hao Su[1,2]
[1] University of California San Diego
[2] Hillbot
{zhl165, z6ling, yuz256, haosu}@ucsd.edu

Abstract

Large Vision-Language Models (LVLMs) have made significant strides in image caption, visual question answering, and robotics by integrating visual and textual information. However, they remain prone to errors in incongruous contexts, where objects appear unexpectedly or are absent when contextually expected. This leads to two key recognition failures: object misidentification and hallucination. To systematically examine this issue, we introduce the ***Object Recognition in Incongruous Context Benchmark (ORIC)****, a novel benchmark that evaluates LVLMs in scenarios where object-context relationships deviate from expectations. ORIC employs two key strategies:* ***(1) LLM-guided sampling****, which identifies objects that are present but contextually incongruous, and* ***(2) CLIP-guided sampling****, which detects plausible yet nonexistent objects that are likely to be hallucinated, thereby creating an incongruous context. Evaluating 18 LVLMs and two open-vocabulary detection models, our results reveal significant recognition gaps, underscoring the challenges posed by contextual incongruity. This work provides critical insights into LVLMs' limitations and encourages further research on context-aware object recognition. The code is available at* https://github.com/ZhaoyangLi-1/ORIC.

1. Introduction

Large Vision-Language Models (LVLMs) have shown strong performance across tasks such as image caption [13], visual question answering [51], robotics [20], and embodied AI [64], enabled by their ability to integrate visual and textual modalities. A core capability underlying these successes is accurate object recognition [10], which supports reliable perception and high-level reasoning [73]. However, despite their overall progress, LVLMs remain prone to two critical recognition failures: **(1) object misidentification**, where existing objects are overlooked [43]; and **(2) object hallucination**, where nonexistent objects are falsely detected [12, 50]. These errors persist even in models achieving high accuracy on standard benchmarks and can severely compromise performance in downstream applications [18, 33].

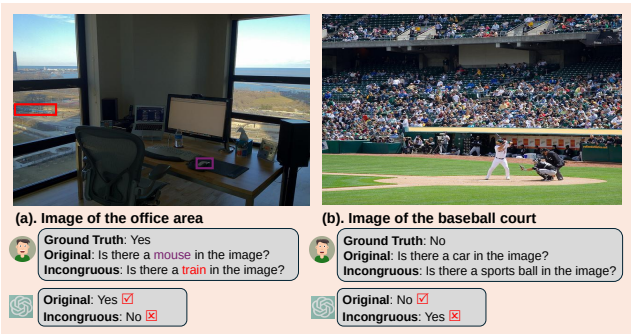

Figure 1. **Contextual Incongruity Leads to Recognition Failures.** This figure illustrates how incongruous contexts cause two primary errors: misidentification of present objects and hallucination of absent ones. **(a) Misidentification:** In an office, GPT-4o identifies the expected "mouse" (purple) but fails to recognize the out-of-context "train" (red). **(b) Hallucination:** On a baseball court, the model correctly denies an unrelated "car" but hallucinates a plausible yet non-existent "sports ball."

Existing benchmarks have made significant progress in evaluating object recognition in LVLMs. One line of work, including POPE [32], AMBER [57], and CIEM [24], assesses recognition based on statistical and textual priors. Another, exemplified by HallusionBench [22] and GVT-bench [57], explores visual semantic consistency. More recent benchmarks have broadened this scope: Hallu-PI [16] examines robustness to low-level pixel perturbations (e.g., noise, blur), while MM-Vet v2 [68] assesses LVLMs' ability to handle sequential image-text inputs. However, despite this broad coverage, a fundamental dimension remains critically underexplored: ***the impact of contextual incongruity on object recognition***.

Contextual incongruity arises when objects appear in

*Equal contribution.

unexpected settings or expected objects are absent from familiar environments. This incongruity significantly impairs LVLMs' ability to correctly identify or dismiss objects, leading to increased object misidentification and hallucination. For example, as illustrated in Fig.1(a), GPT-4o [26] successfully identifies a mouse but fails to recognize a prominent train within an office environment. Similarly, in Fig.1(b), the model correctly rejects the presence of a car but mistakenly identifies a sports ball on a baseball court. These findings suggest that LVLMs' reliance on scene-level contextual priors can bias them against detecting contextually incongruent objects, which aligns with cognitive neuroscience research, showing that unexpected contexts hinder human perception and object recognition [28, 46, 61].

Motivated by this gap, our research systematically investigates how contextual incongruity affects LVLMs' performance. We empirically demonstrate that deviations from expected visual contexts notably degrade the performance of LVLMs in recognizing objects. To methodically explore this phenomenon, we introduce the **Object Recognition in Incongruous Context Benchmark (ORIC)**, specifically designed to assess LVLM performance under incongruous object-background combinations. ORIC employs two novel strategies to create binary classification tasks. **(1) LLM-Guided Sampling:** Leveraging the Large Language Model (LLM), GPT-4o, we identify objects that exist but become challenging to recognize due to their incongruous backgrounds. GPT-4o aids in selecting object-background pairs likely to lead to misidentification. **(2) CLIP-Guided Sampling:** Leveraging CLIP's [48] visual-textual alignment capabilities, we identify plausible yet nonexistent objects strongly suggested by incongruous contexts. This method ranks object candidates based on CLIPScore [23], selecting highly probable but absent objects. We evaluate 18 different LVLMs as well as two open-vocabulary detection models on our ORIC benchmark. Our experiments show that models excelling on standard benchmarks still struggle with ORIC, exposing significant gaps in object recognition under incongruous contexts. In summary, our key contributions are:

- **Problem Identification:** This work pioneers the formal study of contextual incongruity, a critical yet overlooked challenge in LVLMs, systematically demonstrating its significant impact on their object recognition capabilities.
- **A Novel Benchmark:** We introduce **ORIC**, the first benchmark designed to systematically evaluate LVLM object recognition under visual contextual incongruity.
- **Innovative Context-aware Question Construction Methods:** We propose an LLM-guided and CLIP-guided sampling strategy to create challenging recognition tasks.
- **Comprehensive Analysis:** We extensively evaluate multiple LVLMs, highlighting their strengths and limitations.

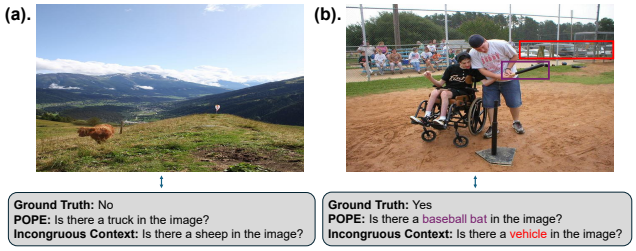

Figure 2. **Comparison of POPE and Incongruous Context Questions.** Both examples use the same image but differ in target objects. **(a)** In a rural scene with a cow, POPE targets a truck, while our question targets a sheep—more contextually plausible but still absent, increasing incongruity. Both answers are "no." **(b)** In a baseball field, POPE targets a baseball bat (purple), while ours targets a large vehicle (red), which is less related to the scene and thus more incongruous. Both answers are "yes."

2. Revisiting POPE: The Role of Contextual Incongruity in Object Recognition

This section revisits the POPE benchmark to assess the impact of incongruous contexts on object recognition. Using CLIPScore [23], we underscore the need for more comprehensive evaluations in these scenarios.

2.1. POPE Limitations in Object Recognition

Recent studies show that LVLMs perform well on benchmarks like POPE, which typically define object recognition as a binary classification task based on the statistical properties of object categories. However, such a purely statistical approach inadequately reflects real-world complexities, especially challenges posed by visual context incongruity. As shown in Fig. 1, POPE overlooks these complexities, revealing key limitations. As a result, it oversimplifies object recognition and fails to reflect real-world performance.

To further explore these limitations, we sampled 25 "yes"-labeled and 25 "no"-labeled POPE questions and revised the objects mentioned to create scenarios featuring visual context incongruity. These questions, termed *incongruous context questions*, maintain original images but introduce unexpected object-context pairs. For example, as depicted in Fig.2(a), a rural scene containing a cow originally queried, *"Is there a truck in the image?"* was modified to *"Is there a sheep in the image?"* Similarly, Fig. 2(b) shows a baseball field where someone is coaching baseball, with the question *"Is there a baseball bat in the image?"* revised to *"Is there a vehicle in the image?"*. These examples clearly introduce higher degrees of visual context incongruity. We evaluate models GPT-4o-08-06 [26], InternVL3-9B [76], Janus-Pro-7B [9], and LLaVA-v1.6-Vicuna-13B [39] using macro accuracy, precision, recall, and F1 score, with detailed formulas in Appendix A.3.

Tab. 1 shows macro Precision, Recall, and F1 scores for four popular models on the POPE subset and incongru-

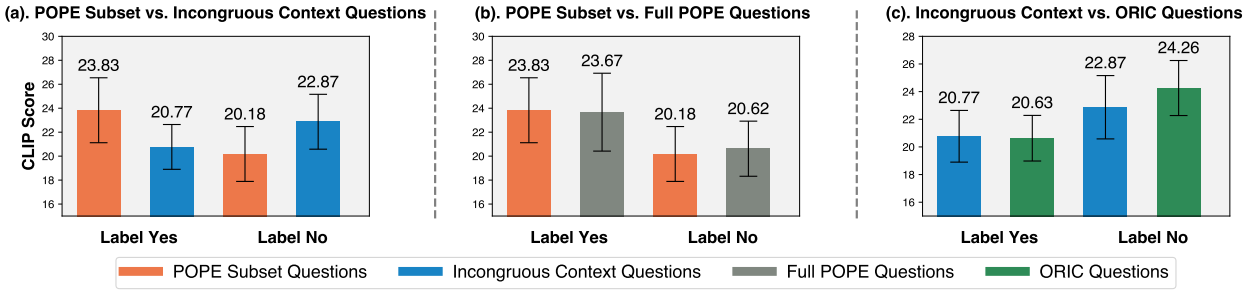

Figure 3. **CLIPScore Analysis of Object-Context Congruity.** CLIPScore (×100) quantifies alignment between queried objects and scene context. **(a)** For "yes" questions, POPE subset yields higher scores than incongruous variants (23.83 vs. 20.77); for "no" questions, the reverse holds (22.87 vs. 20.18), indicating stronger misleading cues. **(b)** The sampled POPE subset shows consistent CLIPScore distribution with the full dataset, confirming its representativeness. **(c)** ORIC questions exhibit even higher incongruity (e.g., 24.26 for "no"), reinforcing the contextual challenge. Subplots (a) and (c) share images but differ in queried objects. Error bars show 95% confidence intervals.

Model	POPE Subset			Incongruous Context		
	Prec.	Rec.	F1.	Prec.	Rec.	F1.
LLaVA-v1.6-13B	98.08	98.00	98.00	58.12	58.00	**57.85**
Janus-Pro-7B	96.30	96.00	95.99	58.01	58.00	**57.98**
InternVL3-9B	100.00	100.00	100.0	56.16	56.00	**58.00**
GPT-4o-0806	100.00	100.00	100.0	61.27	60.32	**60.79**

Table 1. **Model Performance on POPE vs. Incongruous Context Questions.** This table reports macro precision (Prec.), recall (Rec.), and F1 score (F1) for three LVLMs on the POPE benchmark and a set of manually curated questions. Although all models perform well on the POPE subset, they struggle with incongruous context questions.

ous context questions. While GPT-4o-0806 and InternVL3-9B reach perfect scores (100.0) on POPE, LLaVA-v1.6-13B and Janus-Pro-7B also perform strongly with macro F1 scores of 98.0 and around 96.0, respectively. However, performance drops notably in incongruous contexts: GPT-4o-0806 falls to a macro F1 of 60.79, while others drop tod near 58, highlighting LVLMs' challenges with incongruous contexts.

2.2. Quantitative Analysis of Object-Background Associations via CLIPScore

CLIPScore quantifies the semantic alignment between an image and a textual description by computing the cosine similarity of their respective embeddings. It assesses the relevance between the textual description of a specific object and the background information. Specifically, given an image I and a textual question-related object O, the CLIP model [48] computes their embeddings through its visual and textual encoders. The embeddings are normalized as follows: $\hat{f}_I = \frac{f_I}{\|f_I\|}$ and $\hat{f}_O = \frac{f_O}{\|f_O\|}$. The CLIPScore is then calculated as:

$$\text{CLIPScore}(I, O) = \hat{f}_I^\top \hat{f}_O = \frac{f_I^\top f_O}{\|f_I\| \, \|f_O\|} \quad (1)$$

where $f_I, f_O \in \mathbb{R}^d$, and d is the embedding dimensionality. We computed CLIP scores for 50 POPE subset questions and their corresponding incongruous context variants, as shown in Fig. 3(a). For "yes" questions, objects from the original POPE questions show a higher mean CLIP score (23.83) than those in incongruous contexts (20.77), indicating weaker contextual alignment in incongruous settings. Conversely, for "no" questions, incongruous context questions yield higher mean scores (22.87) compared to original POPE questions (20.18). This suggests that incongruous contexts provide stronger contextual cues for nonexistent objects, thereby creating more incongruous visual scenarios due to the absence of the object. The middle subplot in Fig. 3(b) further confirms consistency between the sampled subset and the complete POPE set, validating the representativeness of our selected samples. These findings highlight that POPE neglects the critical influence of incongruous context, emphasizing the necessity for benchmarks like ORIC, which accurately evaluate LVLMs in challenging, real-world scenarios involving contextual incongruity. See Appendix C for details on the CLIPScore discussion.

3. The ORIC benchmark

This section introduces ORIC, a benchmark for evaluating LVLMs' object recognition under contextual incongruity. Formulated as a binary classification task, it assigns each question a "yes" or "no" label based on the target object's presence. As shown in Tab. 2, ORIC uniquely combines contextual incongruity and LLM-free evaluation while assessing both missed and hallucinated recognitions, setting it apart from existing benchmarks. We outline our question construction, statistical analysis, and evaluation protocol.

3.1. ORIC Construction Method

Positive Question (Existing Objects): Contextual incongruity often arises when objects appear in unexpected settings, increasing misidentification risk. Therefore,

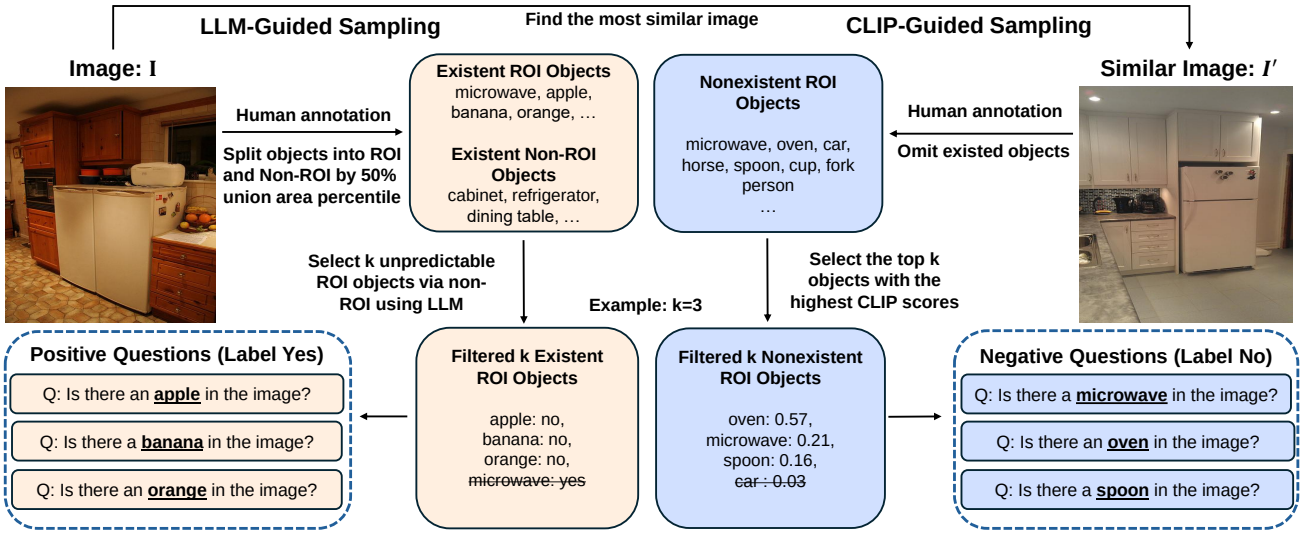

Figure 4. **ORIC Method Overview.** This figure shows two construction methods of the ORIC. **LLM-Guided Sampling (Positive Question Construction):** First, given an image I, objects are classified as ROI if their combined bounding box area is under 50%; otherwise, they are non-ROI. Next, we query the LLM (GPT-4o) with textual categories of non-ROI objects to predict the existence of each ROI object based on common sense and co-occurrence. Finally, we select the top k unpredictable ROI objects (e.g., $k = 3$) for which the LLM predicts "no" (e.g., apple, banana, and orange). **CLIP-Guided Sampling (Negative Question Construction):** A similar image I' is identified using cosine distance from I. We then compute the CLIPScore for each nonexistent ROI object against I' and select the top k nonexistent ROI objects based on their scores. For example, the top three are an oven (0.57), a microwave (0.21), and a spoon (0.16).

Benchmark	Image Count	Contextual Incongruity	LLM-Free Evaluation	Missed / Hallucinated Recognition
HallusionBench	346	✗	✗	Hallucinated only
POPE	500	✗	✓	Both
MM-Vet v2	517	✗	✗	Both
AMBER	1k	✗	✓	Both
Hallu-PI	1.2k	✗	✓	Hallucinated only
ORIC	**1k**	✓	✓	**Both**

Table 2. **Benchmark Comparison.** Benchmarks are compared by image count, contextual incongruity, LLM-free evaluation, and whether both missed and hallucinated object recognitions are assessed.

our objective is to generate questions that deliberately minimize background-object associations, utilizing **LLM-guided sampling**. We define the objects targeted for recognition as ROI (regions of interest), while background contexts consist of non-ROI elements. Formally, as illustrated on the left side of Fig. 4, given an image I containing objects $\mathcal{O} = \{o_i = (n_i, \{B_{ij}\}_{j=1}^{m_i})\}_{i=1}^{N}$, where n_i is the object's name and B_{ij} denotes the j-th bounding box associated with object o_i, we categorize objects into ROI and non-ROI based on their bounding box coverage. We then select k ROI objects as positive question candidates, where k is the desired number of selected objects. The total area covered by each object's bounding boxes is calculated as:

$$A_i = \text{area}\Big(\bigcup_{j=1}^{m_i} B_{ij}\Big), \tag{2}$$

where the function $\text{area}(\cdot)$ computes pixel area, and then we split $\mathcal{O}$ into two disjoint sets based on the $50th$ percentile: $\mathcal{O}_{\text{ROI}} = \{o_{(i)} \mid A_{(i)} < P_{50}(A)\}$ and $\mathcal{O}_{\text{nonROI}} = \{o_{(i)} \mid A_{(i)} \geq P_{50}(A)\}$, where $P_{50}(A)$ represents the median (50th percentile) of the bounding box coverage. We then use GPT-4o as LLM to filter ROI candidates. Specifically, the LLM is queried to determine whether each ROI object is logically consistent with the provided non-ROI object categories. The verification function is defined as:

$$f(o) = \begin{cases} 1, & \text{if LLM}(o, \mathcal{O}_{\text{nonROI}}) = \text{“no”}, \\ 0, & \text{otherwise.} \end{cases} \tag{3}$$

The function $\text{LLM}(o, \mathcal{O}_{\text{nonROI}})$ returns "no" if the ROI object is unexpected based on common sense and typical co-occurrence. Objects receiving a "no" from GPT-4o form the positive candidate set $\mathcal{C}$. Positive questions are generated by randomly selecting k objects from $\mathcal{C}$. For detailed pseudocode and prompts, refer to Appendix A.1.

Negative Question (Nonexistent Objects): LVLMs are prone to object hallucinations when strong contextual cues

make nonexistent objects appear plausible, resulting in incongruous contexts. Therefore, our goal is to generate questions that enhance the correlation between nonexistent ROI objects and non-ROI elements by leveraging **CLIP-guided sampling**. As depicted on the right side of Fig. 4, we first identify the most visually similar image I' to a query image I using the CLIP model's image encoder. Formally, Given images $\{I_1, \ldots, I_n\}$ a query image I_q, visual embeddings are extracted via ViT: $e = ViT(I)$. The image similarity is measured using cosine distance:

$$D(I_q, I_i) = 1 - \frac{\mathbf{e}_q \cdot \mathbf{e}_i}{\|\mathbf{e}_q\| \|\mathbf{e}_i\|}, \tag{4}$$

where $\mathbf{e}_q$ and $\mathbf{e}_i$ represent embeddings of image I_q and I_i, respectively. The most similar image I' minimizes this distance. Next, given the most similar image I' and a set of nonexistent ROI objects $\mathcal{O}_{\text{non}} = \{n_i\}_{i=1}^{M}$, where n_i represents an individual nonexistent ROI object and M is the total number of nonexistent ROI objects considered in the set $\mathcal{O}_{\text{non}}$. For each n_i, a text description T_i is generated in the form of "*an image contains* n_i". We compute the similarity score for each object as $s_i = \text{CLIPScore}(I', T_i)$. The objects are then sorted by s_i, and the top k nonexistent ROI objects are selected to form $\mathcal{O}_{\text{non}}$ for negative question generation. See Appendix A.2 for the detailed algorithm.

3.2. ORIC Statistics

Human Evaluation: We sampled 150 "yes" and 150 "no" questions from ORIC and manually checked **(1)** object labeling and **(2)** visual context incongruity. The low 2% error rate confirms the robustness of our pipeline. Appendix D.1 lists six errors; more examples are in Appendix D.2.

CLIPScore for ROI–Background Analysis: We compared ORIC-generated questions with incongruous context questions in Sec.2 using a CLIPScore-based method. Specifically, we generated 50 ORIC questions (25 for each label, "yes" and "no") corresponding to the same images used in the previous incongruous context questions. As illustrated in Fig.3(c), CLIP scores for "yes" questions were nearly identical between ORIC (20.77) and incongruous context questions (20.63), suggesting similar contextual alignment. However, for "no" questions, ORIC achieved higher CLIP scores (24.25 vs. 22.87), indicating a stronger correlation between the nonexistent object and the visual context, thereby creating a more incongruous context.

Image Similarity Analysis via Minimum Distance: To further characterize the ORIC, we analyzed the visual relationships between positive and negative questions through image similarity measurements. Specifically, for each object class appearing in positive ("yes") questions, we computed its minimum visual distance to negative ("no") questions containing the same object class. Given an object o_i, let the set of positive images be $\mathcal{I}_i^+ = \{I_{i,1}^+, \ldots, I_{i,m}^+\}$ and the set of negative images be $\mathcal{I}_i^- = \{I_{i,1}^-, \ldots, I_{i,n}^-\}$. We extracted visual feature vectors using a ViT encoder and computed pairwise cosine distances as follows:

$$D(I_{i,k}^+, I_{i,l}^-) = 1 - \frac{e(I_{i,k}^+) \cdot e(I_{i,l}^-)}{\|e(I_{i,k}^+)\| \, \|e(I_{i,l}^-)\|} \tag{5}$$

where $e(\cdot) = \text{ViT}(\cdot)$ denotes the ViT feature extractor. The minimum distance between positive and negative sets is defined as $D_{\min} = \min_{k,l} D(I_{i,k}^+, I_{i,l}^-)$. To ensure thorough evaluation, we calculated these minimum distances using three widely used vision encoders commonly employed in encoder-based LVLMs: CLIP-ViT-BigG-P14, SigLIP-SO400M-P14-384 [71], and EVA02-CLIP-BigE-P14 [52]. These analyses highlight the distinctiveness of ORIC in capturing contextually challenging object recognition scenarios compared to existing benchmarks. In Tab. 3, ORIC shows consistently smaller minimum cosine distances between "yes" and "no" samples than POPE across all three vision encoders. This suggests greater visual similarity between positive and negative examples, making object recognition more challenging and realistic.

Vision Encoder	POPE	ORIC
CLIP-ViT-BigG-P14	0.37	**0.14**
SigLIP-SO400M-P14-384	0.28	**0.11**
EVA02-CLIP-BigE-P14	0.40	**0.13**

Table 3. **Comparison of Minimum Cosine Distances.** This table compares the minimum cosine distances between positive and negative questions across three vision encoders. A smaller distance indicates greater semantic similarity between images, meaning "yes" and "no" questions are linked to finer image details and higher representational clutter, making object recognition more challenging and realistic.

3.3. Evaluation Protocol

Answer Matching Method: To accurately interpret ambiguous predictions from LVLMs, we adopt the two-step matching method from MMBench [40]. Initially, heuristic rules attempt to directly extract labels from model predictions. If heuristic methods fail, we prompt GPT-4o-0806 with the original question, the provided answer choices ("yes" or "no"), and the LVLM's prediction, requesting GPT-4o to identify the most appropriate choice.

Evaluation Metrics: ORIC is structured as a balanced binary classification task. We evaluate model performance using several key metrics: the proportion of "yes" predictions, macro precision, macro recall, and macro F1 score. Additionally, we provide precision, recall, and F1 score separately for each class ("yes" and "no") to facilitate a detailed,

Model	Overall				Label Yes			Label No		
	Pre.	Rec.	F1	YP (%)	Pre.	Rec.	F1	Pre.	Rec.	F1
Closed-source										
GPT-4o-2024-08-06	76.14	75.60	**75.45**	54.25	74.06	79.85	**76.61**	78.23	71.35	**74.29**
Vision-encoder-based										
Llama-3.2-11B-Vision	25.00	50.00	33.33	0.00	0.00	0.00	0.00	50.00	100.00	66.67
Chameleon-7B	59.75	50.10	34.08	99.28	50.05	99.38	66.57	69.45	0.82	1.59
BLIP-3	43.14	49.86	42.99	81.54	45.36	51.22	47.02	40.92	48.50	38.96
VILA1.5-13B	65.19	62.40	60.41	28.95	71.44	41.35	51.86	58.92	83.45	68.96
GLM-4v-9B	71.18	64.92	61.99	23.32	82.41	38.25	51.61	59.94	91.60	72.35
Phi-3.5-Vision-Instruct	68.69	68.06	67.79	40.86	72.12	58.92	64.85	65.27	77.20	70.73
InternLM-XComposer2.5-7B	73.32	70.35	69.33	33.77	80.96	54.12	64.17	65.67	86.58	74.49
Qwen2.5-VL-7B-Instruct	75.51	71.67	70.56	30.62	85.39	52.30	64.86	65.63	91.05	76.28
SmolVLM2-2.2B-Instruct	72.87	71.44	70.95	38.01	78.30	59.45	67.38	67.44	83.42	74.52
Kimi-VL-A3B-Instruct	74.67	72.28	71.58	34.45	82.32	56.73	67.13	67.02	87.83	76.02
Molmo-7B-D-0924	78.92	73.74	71.95	69.34	68.22	93.08	76.61	89.62	54.40	65.59
LLaVA-v1.6-Vicuna-13B	75.29	74.56	74.37	56.94	71.76	81.50	76.19	78.82	67.62	72.55
Janus-Pro-7B	76.60	75.22	74.83	56.42	73.30	81.65	**76.71**	79.90	68.80	72.95
InternVL3-9B	77.33	76.95	**76.87**	44.60	80.27	71.55	75.60	74.39	82.35	**78.13**
Vision-encoder-free										
Fuyu-8B	44.83	50.16	34.16	99.29	50.08	99.45	**66.61**	39.59	0.88	1.71
EVE-7B-HD-v1.0	61.02	56.42	51.59	76.53	54.82	82.95	65.27	67.22	29.90	37.90
Emu3-Chat	67.74	65.79	**64.78**	33.41	73.58	49.20	58.90	61.91	82.38	**70.67**
Open-vocabulary Detection										
OWLv2	73.02	72.25	72.02	40.85	77.23	63.10	69.46	68.81	81.40	**74.58**
Grounding DINO 1.5 Pro	77.02	73.40	**72.48**	68.30	67.13	91.70	**77.51**	86.91	55.10	67.44

Table 4. **Main Experimental Results on ORIC.** Performance is broken down by model category and label type (Yes/No). We report macro precision (Prec.), recall (Rec.), F1 score, and the proportion of "yes" predictions (YP). Results for LVLMs are averaged over four prompts, while detection models use a single prompt. Full metric definitions are in Appendix A.3.

class-wise analysis of model behavior. For further information on these metrics, please refer to Appendix A.3.

4. Experiments and Analysis

We evaluate **18** LVLMs and **2** open-vocabulary detection models on the ORIC (Sec. 4.1), with supplementary experiments and analysis (Sec.4.2).

4.1. Main ORIC Experiment

We present the main experimental settings, including ORIC benchmark setup, evaluated models, evaluation protocols, prompting, input preprocessing, and result analysis.

4.1.1. Experimental Setup

ORIC Setup: We evaluate performance on the ORIC benchmark (constructed as detailed in Sec.3.1), comprising 1000 images sampled from the MSCOCO [37] validation set to avoid data leakage. Each pair includes one image containing two existing objects and another with two non-existing objects, resulting in $1,000$ 'yes"-label and 1,000 no"-label questions for evaluating object recognition.

Evaluated Models: We evaluate **18** widely used LVLMs, covering vision-encoder-based models, vision-encoder-free models, and closed-source models. Additionally, we assess open-vocabulary detection models, such as Grounding DINO 1.5 Pro [49] and OWLv2 [44], for auxiliary comparison. Full model details are provided in Appendix B.1.

Evaluation Configuration: We maintain consistent settings for both LVLMs and detection models, conducting all experiments on a single NVIDIA H100 GPU. We set the temperature to 0 for deterministic outputs and limit generation to 1,024 tokens. For open-vocabulary detection models, we jointly process present and absent objects for efficient evaluation. A model answers "yes" if it detects at least one instance with a confidence score of 0.25; otherwise, it answers "no." We query LVLMs using four distinct prompts and compute the mean metrics as described in Sec. 3.3. In contrast, Grounding DINO 1.5 Pro and OWLv2 follow their own established prompts, eliminating the need to compute mean metrics. Appendix B.2 provides further details on LVLMs and open-vocabulary prompts.

4.1.2. Main Results and Analysis

Tab. 4 presents the performance of 18 LVLMs and 2 open-vocabulary detection models on the ORIC benchmark. We analyze overall performance, architecture differences, and the impact of incongruous context.

Overall Performance: Top-performing models included both vision-encoder-based and closed-source models, such as InternVL3-9B (F1: 76.87), GPT-4o (75.45), Janus-Pro-7B (74.83), and LLaVA-v1.6-13B (74.37), showing greater robustness to contextual incongruity than other LVLMs and detection models. Still, most models score between 60 and 77 in macro F1, highlighting ORIC's challenge. Notably, Llama-3.2-11B-Vision and Chameleon-7B fail drastically. Models like GLM-4v-9B and Molmo-7B-D-0924 show precision exceeding recall by over 5 points, indicating missed objects. In contrast, Fuyu-8B and BLIP-3 show recall significantly higher than precision, suggesting hallucinations. Even accounting for possible data leakage, the top score of 76.87 (InternVL3-9B) confirms that LVLMs remain limited in recognizing objects in incongruous contexts.

Model Architecture Comparison: Vision-encoder-based models like InternVL3-9B and Janus-Pro-7B outperform encoder-free models, with Emu3—the best among the latter—achieving only 64.78 F1. This performance gap likely arises from ViT-style encoders' ability to extract structured visual features, enhancing fine-grained object perception. In contrast, encoder-free models like Fuyu-8B process raw pixels, making them more susceptible to spatial detail loss in complex scenes. GPT-4o scores 75.45 F1, falling short of InternVL3-9B by 1.42 points—highlighting that open-source models can not only rival but also surpass closed-source ones. Meanwhile, open-vocabulary detectors (e.g., OWLv2, Grounding DINO 1.5 Pro) lag behind LVLMs due to their reliance on region-text alignment without modeling object absence or global context. Their lack of holistic reasoning and negative evidence leads to frequent hallucinations in incongruous scenes, limiting robustness.

Influence of Incongruous Context (Class-Wise): While GPT-4o and InternVL3-9B maintain strong F1 scores across both "yes" and "no" labels, our analysis reveals how contextual incongruity affects object recognition errors across models. For "yes"-label questions, models frequently misidentify objects due to mismatched backgrounds. GLM-4v-9B and LLaMA-3.2-11B-Vision often reject valid objects, resulting in low "yes" recall and F1 scores. Similarly, OWLv2 struggles in incongruous scenes, exhibiting poor "yes" recall. In contrast, Molmo-7B tends to ignore contextual cues and over-rely on local object features. For "no"-label questions, many models hallucinate plausible-but-absent objects—especially those sensitive to background signals. Chameleon-7B, VILA1.5-3B, and BLIP-3 frequently misclassify such objects as present, yielding high "yes" rates but poor "no" recall. Detection models like Grounding DINO face similar challenges, with notably low "no" precision. Overall, most LVLMs and open-vocabulary detection models suffer from object hallucination and misidentification in ORIC, highlighting the challenge of recognizing objects in the incongruous context.

4.2. Supplementary Experiments and Analysis

We follow the main ORIC experiment settings, averaging LVLM metrics over four prompts and using a default prompt for detection models.

Model	Random	Pos Only	Neg Only
DINO 1.5 Pro	95.50 / 85.50	91.60 (-3.90)	53.05 **(-32.45)**
GPT-4o-0806	85.90 / 85.67	79.60 (-6.30)	71.65 (-14.02)
Emu3	67.25 / 97.30	48.75 **(-18.50)**	81.17 (-16.13)
Janus-Pro-7B	88.05 / 88.75	81.97 (-6.08)	67.40 (-21.35)
InternVL3-9B	80.88 / 97.83	68.83 (-12.05)	81.75 (-16.08)

Table 5. **Ablation study of ORIC's construction methods.** The table evaluates three sampling setups: **Random:** A baseline using randomly selected positive and negative objects. **Pos Only:** Employs LLM-guided sampling for positives and random negatives. **Neg Only:** Uses CLIP-guided sampling for negatives and random positives. All values are reported as (yes-recall / no-recall), with parentheses indicating the performance drop relative to the Random baseline.

ORIC Ablation Study: Tab. 5 shows that both LLM-guided and CLIP-guided sampling increase question difficulty across four LVLMs and Grounding DINO Pro 1.5. LLM-guided sampling reduces yes-recall across all models, with Emu3 experiencing the largest drop (-18.50). Meanwhile, CLIP-guided sampling significantly lowers no-recall, with the most notable decline observed in DINO 1.5 Pro (-32.45). These results suggest that both positive and negative question constructions introduce challenges, though their effects differ. Notably, no-recall declines more sharply in most models. This discrepancy arises because positive questions reference real objects, aiding recognition even in incongruous backgrounds, whereas negative questions involve absent objects, leading models to over-rely on background context and hallucinate in congruous settings.

Beyond POPE, Increased Challenge: To assess the impact of contextual incongruity, we compare ORIC with the prior POPE benchmark, both of which contain a balanced set of 2,000 questions. As shown in Tab. 6, five models that performed well on POPE show significantly lower macro F1 scores on our benchmark, with performance gaps across

Model	POPE			ORIC		
	Prec.	Rec.	F1.	Prec.	Rec.	F1.
Emu3-Chat	87.38	86.72	86.65	67.74	65.79	64.78
DINO 1.5 Pro	85.62	85.05	84.99	77.02	73.40	72.48
Janus-Pro-7B	87.32	87.03	87.00	76.60	75.22	74.83
GPT-4o-0806	86.78	86.75	86.75	76.14	75.60	75.45
InternVL3-9B	88.8	88.69	**88.68**	77.33	76.95	**76.87**

Table 6. **Model Performance on POPE vs. ORIC.** Comparison of POPE and ORIC, both with 2000 balanced questions across five models. We report macro precision (Prec.), recall (Rec.), and F1 score (F1) for four LVLMs and one detection model, showing that ORIC poses a greater challenge.

models becoming more pronounced. Notably, GPT-4o-0806 exhibits the smallest macro F1 drop (11.3), highlighting its robustness. A full comparison across 18 LVLMs and two open-vocabulary detectors is provided in Appendix B.3.

Performance Comparison Across Object Sizes: We adopt COCO's size tiers—small ($< 24^2$ pt^2), medium (24–96^2 pt^2), and large ($\geq 96^2$ pt^2)—to compare POPE and ORIC on 1,000 "yes"-labeled questions from each. All four models exhibit lower recall on ORIC, with an average drop of 13.51 points across sizes. Emu3-Chat performs worst, particularly on small objects (68.22 $\rightarrow$ 38.73, –29.49), while GPT-4o-0806 is most robust on large ones (–7.59). Notably, Emu3-Chat's large–small gap widens from 25.97 in POPE to 33.26 in ORIC, and InternVL3-9B's from 14.05 to 22.82. Although large objects remain easier to recognize, the consistent decline across all sizes suggests that incongruous context—rather than object scale—is the primary cause of performance degradation. Object size distributions for POPE, ORIC, and COCO are shown in Appendix B.4.

Model	POPE			ORIC		
	Small	Medium	Large	Small	Medium	Large
Emu3-Chat	68.22	80.97	94.19	38.73	56.61	71.99
InternVL3-9B	82.29	90.43	96.34	63.63	77.61	86.45
GPT-4o-0806	82.89	89.40	94.94	77.52	81.03	**87.35**
Janus-Pro-7B	**83.70**	**93.21**	**96.51**	**78.40**	**84.22**	**87.35**

Table 7. **Recall by Object Size on POPE vs. ORIC.** We report the recall for questions labeled "yes" across small, medium, and large objects in both the POPE and ORIC datasets for three LVLMs, illustrating how object scale affects model performance.

Evaluation with Chain-of-Thought (CoT): We evaluate the top four LVLMs, representing the three major LVLM categories, using zero-shot CoT prompting [60] under the same settings as the main experiment on ORIC, except that we adopt the zero-shot CoT prompt detailed in Appendix B.2. As shown in Fig. 5, CoT prompting does not consistently improve performance on incongruous context tasks, due to the limited fine-grained visual perception capabilities of current LVLMs, further underscoring the challenges posed by our benchmark.

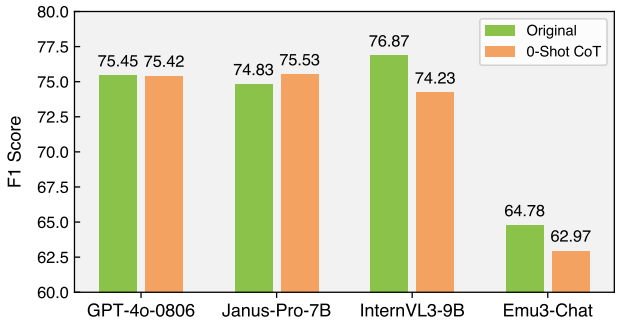

Figure 5. **Zero-shot CoT Prompting Performance on ORIC.** Macro F1 scores of four top-performing LVLMs under original and zero-shot CoT prompting settings.

5. Related Work

Large Vision-Language Models: Recent advances in large vision-language models (LVLMs) have greatly enhanced text-image processing for visual understanding [1, 26, 58, 75]. These models fall into two categories: vision-encoder-based approaches [2, 3, 21, 31, 38], which use pretrained visual encoders like Vision Transformer (ViT) [17], and vision-encoder-free methods [6, 15, 59], which tokenize image patches for joint text-image processing. LVLMs are widely used in tasks such as image captioning [13], visual question answering [51], robotics [20, 25, 45], and embodied AI [64, 72]. Despite progress, they still struggle with fine-grained perception, particularly in recognizing object attributes and relationships [47].

Benchmarking Large Vision-Language Models: As LVLMs evolve, benchmarking is crucial for guiding their development [8, 34, 35]. Various benchmarks assess fine-grained perception, including object counting, relationships, attributes, reasoning [19, 30, 40, 41, 62, 66, 67], and commonsense knowledge [7, 69]. Others evaluate object hallucination and recognition [24, 32, 50, 57], with HALLUCINOGEN [22] focusing on textual influences. Additionally, [22, 55, 56] examine visual semantics in LVLMs, but existing benchmarks overlook background cues in object recognition. To bridge this gap, we introduce ORIC to evaluate recognition under contextual incongruity.

6. Conclusion and Limitations

This paper provides the first systematic investigation into the impact of contextual incongruity on LVLM object recognition, a critical yet largely overlooked problem. We find that even state-of-the-art models are highly susceptible to misidentification and hallucination when visual scenes

violate common-sense expectations. To address this, we introduce ORIC, the first benchmark engineered to specifically test object recognition in incongruous contexts. ORIC is built upon a novel sampling strategy that combines LLM and CLIP guidance to generate challenging, context-aware recognition tasks. Our extensive evaluation of 20 models confirms that robustly handling incongruous contexts remains a significant hurdle for current LVLMs, offering deeper insights into the complexity of this challenge. While our work provides this crucial foundation, we acknowledge its limitations, primarily the reliance on a single dataset. Future research should explore more diverse datasets and develop novel methods to mitigate contextual failures.

References

[1] Marah Abdin, Jyoti Aneja, Hany Awadalla, Ahmed Awadallah, Ammar Ahmad Awan, Nguyen Bach, Amit Bahree, Arash Bakhtiari, Jianmin Bao, Harkirat Behl, et al. Phi-3 technical report: A highly capable language model locally on your phone. *arXiv preprint arXiv:2404.14219*, 2024. 8, 13

[2] Jean-Baptiste Alayrac, Jeff Donahue, Pauline Luc, Antoine Miech, Iain Barr, Yana Hasson, Karel Lenc, Arthur Mensch, Katherine Millican, Malcolm Reynolds, et al. Flamingo: a visual language model for few-shot learning. *Advances in neural information processing systems*, 35:23716–23736, 2022. 8

[3] Jinze Bai, Shuai Bai, Shusheng Yang, Shijie Wang, Sinan Tan, Peng Wang, Junyang Lin, Chang Zhou, and Jingren Zhou. Qwen-vl: A versatile vision-language model for understanding, localization, text reading, and beyond. *arXiv preprint arXiv:2308.12966*, 1(2):3, 2023. 8

[4] Shuai Bai, Keqin Chen, Xuejing Liu, Jialin Wang, Wenbin Ge, Sibo Song, Kai Dang, Peng Wang, Shijie Wang, Jun Tang, Humen Zhong, Yuanzhi Zhu, Mingkun Yang, Zhaohai Li, Jianqiang Wan, Pengfei Wang, Wei Ding, Zheren Fu, Yiheng Xu, Jiabo Ye, Xi Zhang, Tianbao Xie, Zesen Cheng, Hang Zhang, Zhibo Yang, Haiyang Xu, and Junyang Lin. Qwen2.5-vl technical report. *arXiv preprint arXiv:2502.13923*, 2025. 13

[5] Rohan Bavishi, Erich Elsen, Curtis Hawthorne, Maxwell Nye, Augustus Odena, Arushi Somani, and Sağnak Taşırlar. Introducing our multimodal models, 2023. 13

[6] Rohan Bavishi, Erich Elsen, Curtis Hawthorne, Maxwell Nye, Augustus Odena, Arushi Somani, and Sagnak Tasırlar. Introducing our multimodal models, 2023. 8

[7] Nitzan Bitton-Guetta, Aviv Slobodkin, Aviya Maimon, Eliya Habba, Royi Rassin, Yonatan Bitton, Idan Szpektor, Amir Globerson, and Yuval Elovici. Visual riddles: a commonsense and world knowledge challenge for large vision and language models. *arXiv preprint arXiv:2407.19474*, 2024. 8

[8] Lin Chen, Jinsong Li, Xiaoyi Dong, Pan Zhang, Yuhang Zang, Zehui Chen, Haodong Duan, Jiaqi Wang, Yu Qiao, Dahua Lin, et al. Are we on the right way for evaluating large vision-language models? *arXiv preprint arXiv:2403.20330*, 2024. 8

[9] Xiaokang Chen, Zhiyu Wu, Xingchao Liu, Zizheng Pan, Wen Liu, Zhenda Xie, Xingkai Yu, and Chong Ruan. Janus-pro: Unified multimodal understanding and generation with data and model scaling. *arXiv preprint arXiv:2501.17811*, 2025. 2, 13

[10] Zhe Chen, Jiannan Wu, Wenhai Wang, Weijie Su, Guo Chen, Sen Xing, Muyan Zhong, Qinglong Zhang, Xizhou Zhu, Lewei Lu, et al. Internvl: Scaling up vision foundation models and aligning for generic visual-linguistic tasks. In *Proceedings of the IEEE/CVF Conference on Computer Vision and Pattern Recognition*, pages 24185–24198, 2024. 1

[11] Jianfeng Chi, Ujjwal Karn, Hongyuan Zhan, Eric Smith, Javier Rando, Yiming Zhang, Kate Plawiak, Zacharie Delpierre Coudert, Kartikeya Upasani, and Mahesh Pasupuleti. Llama guard 3 vision: Safeguarding human-ai image understanding conversations, 2024. 13

[12] Wenliang Dai, Zihan Liu, Ziwei Ji, Dan Su, and Pascale Fung. Plausible may not be faithful: Probing object hallucination in vision-language pre-training. *arXiv preprint arXiv:2210.07688*, 2022. 1

[13] Wenliang Dai, Junnan Li, Dongxu Li, Anthony Meng Huat Tiong, Junqi Zhao, Weisheng Wang, Boyang Li, Pascale Fung, and Steven Hoi. Instructblip: Towards general-purpose vision-language models with instruction tuning. *arXiv preprint arXiv:2305.06500*, 2023. 1, 8

[14] Matt Deitke, Christopher Clark, Sangho Lee, Rohun Tripathi, Yue Yang, Jae Sung Park, Mohammadreza Salehi, Niklas Muennighoff, Kyle Lo, Luca Soldaini, et al. Molmo and pixmo: Open weights and open data for state-of-the-art multimodal models. *arXiv preprint arXiv:2409.17146*, 2024. 13

[15] Haiwen Diao, Yufeng Cui, Xiaotong Li, Yueze Wang, Huchuan Lu, and Xinlong Wang. Unveiling encoder-free vision-language models. *arXiv preprint arXiv:2406.11832*, 2024. 8, 13

[16] Peng Ding, Jingyu Wu, Jun Kuang, Dan Ma, Xuezhi Cao, Xunliang Cai, Shi Chen, Jiajun Chen, and Shujian Huang. Hallu-pi: Evaluating hallucination in multi-modal large language models within perturbed inputs. In *Proceedings of the 32nd ACM International Conference on Multimedia*, pages 10707–10715, 2024. 1

[17] Alexey Dosovitskiy. An image is worth 16x16 words: Transformers for image recognition at scale. *arXiv preprint arXiv:2010.11929*, 2020. 8

[18] Jiafei Duan, Wilbert Pumacay, Nishanth Kumar, Yi Ru Wang, Shulin Tian, Wentao Yuan, Ranjay Krishna, Dieter Fox, Ajay Mandlekar, and Yijie Guo. Aha: A vision-language-model for detecting and reasoning over failures in robotic manipulation. *arXiv preprint arXiv:2410.00371*, 2024. 1

[19] Chaoyou Fu, Peixian Chen, Yunhang Shen, Yulei Qin, Mengdan Zhang, Xu Lin, Jinrui Yang, Xiawu Zheng, Ke Li, Xing Sun, et al. Mme: A comprehensive evaluation benchmark for multimodal large language models. *arXiv preprint arXiv:2306.13394*, 2023. 8

[20] Jensen Gao, Bidipta Sarkar, Fei Xia, Ted Xiao, Jiajun Wu, Brian Ichter, Anirudha Majumdar, and Dorsa Sadigh. Phys-

ically grounded vision-language models for robotic manipulation. In *2024 IEEE International Conference on Robotics and Automation (ICRA)*, pages 12462–12469. IEEE, 2024. 1, 8

[21] Team GLM, Aohan Zeng, Bin Xu, Bowen Wang, Chenhui Zhang, Da Yin, Diego Rojas, Guanyu Feng, Hanlin Zhao, Hanyu Lai, Hao Yu, Hongning Wang, Jiadai Sun, Jiajie Zhang, Jiale Cheng, Jiayi Gui, Jie Tang, Jing Zhang, Juanzi Li, Lei Zhao, Lindong Wu, Lucen Zhong, Mingdao Liu, Minlie Huang, Peng Zhang, Qinkai Zheng, Rui Lu, Shuaiqi Duan, Shudan Zhang, Shulin Cao, Shuxun Yang, Weng Lam Tam, Wenyi Zhao, Xiao Liu, Xiao Xia, Xiaohan Zhang, Xiaotao Gu, Xin Lv, Xinghan Liu, Xinyi Liu, Xinyue Yang, Xixuan Song, Xunkai Zhang, Yifan An, Yifan Xu, Yilin Niu, Yuantao Yang, Yueyan Li, Yushi Bai, Yuxiao Dong, Zehan Qi, Zhaoyu Wang, Zhen Yang, Zhengxiao Du, Zhenyu Hou, and Zihan Wang. Chatglm: A family of large language models from glm-130b to glm-4 all tools, 2024. 8, 13

[22] Tianrui Guan, Fuxiao Liu, Xiyang Wu, Ruiqi Xian, Zongxia Li, Xiaoyu Liu, Xijun Wang, Lichang Chen, Furong Huang, Yaser Yacoob, et al. Hallusionbench: an advanced diagnostic suite for entangled language hallucination and visual illusion in large vision-language models. In *Proceedings of the IEEE/CVF Conference on Computer Vision and Pattern Recognition*, pages 14375–14385, 2024. 1, 8

[23] Jack Hessel, Ari Holtzman, Maxwell Forbes, Ronan Le Bras, and Yejin Choi. Clipscore: A reference-free evaluation metric for image captioning. *arXiv preprint arXiv:2104.08718*, 2021. 2

[24] Hongyu Hu, Jiyuan Zhang, Minyi Zhao, and Zhenbang Sun. Ciem: Contrastive instruction evaluation method for better instruction tuning. *arXiv preprint arXiv:2309.02301*, 2023. 1, 8

[25] Wenlong Huang, Chen Wang, Ruohan Zhang, Yunzhu Li, Jiajun Wu, and Li Fei-Fei. Voxposer: Composable 3d value maps for robotic manipulation with language models. *arXiv preprint arXiv:2307.05973*, 2023. 8

[26] Aaron Hurst, Adam Lerer, Adam P Goucher, Adam Perelman, Aditya Ramesh, Aidan Clark, AJ Ostrow, Akila Welihinda, Alan Hayes, Alec Radford, et al. Gpt-4o system card. *arXiv preprint arXiv:2410.21276*, 2024. 2, 8, 13

[27] Kiyoon Jeong, Woojun Lee, Woongchan Nam, Minjeong Ma, and Pilsung Kang. Technical report of nice challenge at cvpr 2024: caption re-ranking evaluation using ensembled clip and consensus scores. In *Proceedings of the IEEE/CVF Conference on Computer Vision and Pattern Recognition*, pages 7366–7372, 2024. 16

[28] Olivier R Joubert, Denis Fize, Guillaume A Rousselet, and Michele Fabre-Thorpe. Early interference of context congruence on object processing in rapid visual categorization of natural scenes. *Journal of Vision*, 8(13):11–11, 2008. 2

[29] Martha Lewis, Nihal V Nayak, Peilin Yu, Qinan Yu, Jack Merullo, Stephen H Bach, and Ellie Pavlick. Does clip bind concepts? probing compositionality in large image models. *arXiv preprint arXiv:2212.10537*, 2022. 15

[30] Bo Li, Peiyuan Zhang, Jingkang Yang, Yuanhan Zhang, Fanyi Pu, and Ziwei Liu. Otterhd: A high-resolution multimodality model. *arXiv preprint arXiv:2311.04219*, 2023. 8

[31] Junnan Li, Dongxu Li, Caiming Xiong, and Steven Hoi. Blip: Bootstrapping language-image pre-training for unified vision-language understanding and generation. In *International conference on machine learning*, pages 12888–12900. PMLR, 2022. 8

[32] Yifan Li, Yifan Du, Kun Zhou, Jinpeng Wang, Wayne Xin Zhao, and Ji-Rong Wen. Evaluating object hallucination in large vision-language models. *arXiv preprint arXiv:2305.10355*, 2023. 1, 8

[33] Zongxia Li, Xiyang Wu, Hongyang Du, Huy Nghiem, and Guangyao Shi. Benchmark evaluations, applications, and challenges of large vision language models: A survey. *arXiv preprint arXiv:2501.02189*, 2025. 1

[34] Paul Pu Liang, Akshay Goindani, Talha Chafekar, Leena Mathur, Haofei Yu, Ruslan Salakhutdinov, and Louis-Philippe Morency. Hemm: Holistic evaluation of multimodal foundation models. *arXiv preprint arXiv:2407.03418*, 2024. 8

[35] Zijing Liang, Yanjie Xu, Yifan Hong, Penghui Shang, Qi Wang, Qiang Fu, and Ke Liu. A survey of multimodel large language models. In *Proceedings of the 3rd International Conference on Computer, Artificial Intelligence and Control Engineering*, pages 405–409, 2024. 8

[36] Ji Lin, Hongxu Yin, Wei Ping, Yao Lu, Pavlo Molchanov, Andrew Tao, Huizi Mao, Jan Kautz, Mohammad Shoeybi, and Song Han. Vila: On pre-training for visual language models, 2023. 13

[37] Tsung-Yi Lin, Michael Maire, Serge Belongie, James Hays, Pietro Perona, Deva Ramanan, Piotr Dollár, and C Lawrence Zitnick. Microsoft coco: Common objects in context. In *Computer Vision–ECCV 2014: 13th European Conference, Zurich, Switzerland, September 6-12, 2014, Proceedings, Part V 13*, pages 740–755. Springer, 2014. 6

[38] Haotian Liu, Chunyuan Li, Yuheng Li, and Yong Jae Lee. Improved baselines with visual instruction tuning. In *Proceedings of the IEEE/CVF Conference on Computer Vision and Pattern Recognition*, pages 26296–26306, 2024. 8

[39] Haotian Liu, Chunyuan Li, Yuheng Li, Bo Li, Yuanhan Zhang, Sheng Shen, and Yong Jae Lee. Llava-next: Improved reasoning, ocr, and world knowledge, 2024. 2, 13

[40] Yuan Liu, Haodong Duan, Yuanhan Zhang, Bo Li, Songyang Zhang, Wangbo Zhao, Yike Yuan, Jiaqi Wang, Conghui He, Ziwei Liu, et al. Mmbench: Is your multi-modal model an all-around player? In *European conference on computer vision*, pages 216–233. Springer, 2024. 5, 8

[41] Pan Lu, Swaroop Mishra, Tanglin Xia, Liang Qiu, Kai-Wei Chang, Song-Chun Zhu, Oyvind Tafjord, Peter Clark, and Ashwin Kalyan. Learn to explain: Multimodal reasoning via thought chains for science question answering. *Advances in Neural Information Processing Systems*, 35:2507–2521, 2022. 8

[42] Andrés Marafioti, Orr Zohar, Miquel Farré, Merve Noyan, Elie Bakouch, Pedro Cuenca, Cyril Zakka, Loubna Ben Allal, Anton Lozhkov, Nouamane Tazi, Vaibhav Srivastav, Joshua Lochner, Hugo Larcher, Mathieu Morlon, Lewis Tunstall, Leandro von Werra, and Thomas Wolf. Smolvlm: Redefining small and efficient multimodal models. *arXiv preprint arXiv:2504.05299*, 2025. 13

[43] Dimity Miller, Niko Sünderhauf, Alex Kenna, and Keita Mason. Open-set recognition in the age of vision-language models. In *European Conference on Computer Vision*, pages 1–18. Springer, 2024. 1

[44] Matthias Minderer, Alexey Gritsenko, and Neil Houlsby. Scaling open-vocabulary object detection. *Advances in Neural Information Processing Systems*, 36, 2024. 6, 13

[45] Soroush Nasiriany, Fei Xia, Wenhao Yu, Ted Xiao, Jacky Liang, Ishita Dasgupta, Annie Xie, Danny Driess, Ayzaan Wahid, Zhuo Xu, et al. Pivot: Iterative visual prompting elicits actionable knowledge for vlms. *arXiv preprint arXiv:2402.07872*, 2024. 8

[46] Marius V Peelen, Eva Berlot, Floris P de Lange, and Michele Fabre-Thorpe. Predictive processing of scenes and objects. *Nature Reviews Psychology*, 3(1):13–26, 2024. 2

[47] Wujian Peng, Sicheng Xie, Zuyao You, Shiyi Lan, and Zuxuan Wu. Synthesize diagnose and optimize: Towards fine-grained vision-language understanding. In *Proceedings of the IEEE/CVF Conference on Computer Vision and Pattern Recognition*, pages 13279–13288, 2024. 8

[48] Alec Radford, Jong Wook Kim, Chris Hallacy, Aditya Ramesh, Gabriel Goh, Sandhini Agarwal, Girish Sastry, Amanda Askell, Pamela Mishkin, Jack Clark, et al. Learning transferable visual models from natural language supervision. In *International conference on machine learning*, pages 8748–8763. PMLR, 2021. 2, 3

[49] Tianhe Ren, Qing Jiang, Shilong Liu, Zhaoyang Zeng, Wenlong Liu, Han Gao, Hongjie Huang, Zhengyu Ma, Xiaoke Jiang, Yihao Chen, et al. Grounding dino 1.5: Advance the" edge" of open-set object detection. *arXiv preprint arXiv:2405.10300*, 2024. 6, 13

[50] Anna Rohrbach, Lisa Anne Hendricks, Kaylee Burns, Trevor Darrell, and Kate Saenko. Object hallucination in image captioning. *arXiv preprint arXiv:1809.02156*, 2018. 1, 8

[51] Haoyu Song, Li Dong, Wei-Nan Zhang, Ting Liu, and Furu Wei. Clip models are few-shot learners: Empirical studies on vqa and visual entailment. *arXiv preprint arXiv:2203.07190*, 2022. 1, 8

[52] Quan Sun, Yuxin Fang, Ledell Wu, Xinlong Wang, and Yue Cao. Eva-clip: Improved training techniques for clip at scale. *arXiv preprint arXiv:2303.15389*, 2023. 5

[53] Chameleon Team. Chameleon: Mixed-modal early-fusion foundation models. *arXiv preprint arXiv:2405.09818*, 2024. 13

[54] Kimi Team, Angang Du, Bohong Yin, Bowei Xing, Bowen Qu, Bowen Wang, Cheng Chen, Chenlin Zhang, Chenzhuang Du, Chu Wei, et al. Kimi-vl technical report. *arXiv preprint arXiv:2504.07491*, 2025. 13

[55] Shengbang Tong, Zhuang Liu, Yuexiang Zhai, Yi Ma, Yann LeCun, and Saining Xie. Eyes wide shut? exploring the visual shortcomings of multimodal llms. In *Proceedings of the IEEE/CVF Conference on Computer Vision and Pattern Recognition*, pages 9568–9578, 2024. 8

[56] Guangzhi Wang, Yixiao Ge, Xiaohan Ding, Mohan Kankanhalli, and Ying Shan. What makes for good visual tokenizers for large language models? *arXiv preprint arXiv:2305.12223*, 2023. 8

[57] Junyang Wang, Yuhang Wang, Guohai Xu, Jing Zhang, Yukai Gu, Haitao Jia, Ming Yan, Ji Zhang, and Jitao Sang. An llm-free multi-dimensional benchmark for mllms hallucination evaluation. *arXiv preprint arXiv:2311.07397*, 2023. 1, 8

[58] Peng Wang, Shuai Bai, Sinan Tan, Shijie Wang, Zhihao Fan, Jinze Bai, Keqin Chen, Xuejing Liu, Jialin Wang, Wenbin Ge, Yang Fan, Kai Dang, Mengfei Du, Xuancheng Ren, Rui Men, Dayiheng Liu, Chang Zhou, Jingren Zhou, and Junyang Lin. Qwen2-vl: Enhancing vision-language model's perception of the world at any resolution. *arXiv preprint arXiv:2409.12191*, 2024. 8

[59] Xinlong Wang, Xiaosong Zhang, Zhengxiong Luo, Quan Sun, Yufeng Cui, Jinsheng Wang, Fan Zhang, Yueze Wang, Zhen Li, Qiying Yu, et al. Emu3: Next-token prediction is all you need. *arXiv preprint arXiv:2409.18869*, 2024. 8, 13

[60] Jason Wei, Xuezhi Wang, Dale Schuurmans, Maarten Bosma, Fei Xia, Ed Chi, Quoc V Le, Denny Zhou, et al. Chain-of-thought prompting elicits reasoning in large language models. *Advances in neural information processing systems*, 35:24824–24837, 2022. 8

[61] Miles Wischnewski, Marius V Peelen, Michele Fabre-Thorpe, and Michele Fabre-Thorpe. Causal neural mechanisms of context-based object recognition. *Elife*, 10:e69736, 2021. 2

[62] Shujin Wu, Yi R Fung, Sha Li, Yixin Wan, Kai-Wei Chang, and Heng Ji. Macaroon: Training vision-language models to be your engaged partners. *arXiv preprint arXiv:2406.14137*, 2024. 8

[63] Le Xue, Manli Shu, Anas Awadalla, Jun Wang, An Yan, Senthil Purushwalkam, Honglu Zhou, Viraj Prabhu, Yutong Dai, Michael S Ryoo, et al. xgen-mm (blip-3): A family of open large multimodal models. *arXiv preprint arXiv:2408.08872*, 2024. 13

[64] Jingkang Yang, Yuhao Dong, Shuai Liu, Bo Li, Ziyue Wang, Haoran Tan, Chencheng Jiang, Jiamu Kang, Yuanhan Zhang, Kaiyang Zhou, et al. Octopus: Embodied vision-language programmer from environmental feedback. In *European Conference on Computer Vision*, pages 20–38. Springer, 2024. 1, 8

[65] Suorong Yang, Peng Ye, Wanli Ouyang, Dongzhan Zhou, and Furao Shen. A clip-powered framework for robust and generalizable data selection. *arXiv preprint arXiv:2410.11215*, 2024. 16

[66] Kaining Ying, Fanqing Meng, Jin Wang, Zhiqian Li, Han Lin, Yue Yang, Hao Zhang, Wenbo Zhang, Yuqi Lin, Shuo Liu, et al. Mmt-bench: A comprehensive multimodal benchmark for evaluating large vision-language models towards multitask agi. *arXiv preprint arXiv:2404.16006*, 2024. 8

[67] Weihao Yu, Zhengyuan Yang, Linjie Li, Jianfeng Wang, Kevin Lin, Zicheng Liu, Xinchao Wang, and Lijuan Wang. Mm-vet: Evaluating large multimodal models for integrated capabilities. *arXiv preprint arXiv:2308.02490*, 2023. 8

[68] Weihao Yu, Zhengyuan Yang, Lingfeng Ren, Linjie Li, Jianfeng Wang, Kevin Lin, Chung-Ching Lin, Zicheng Liu, Lijuan Wang, and Xinchao Wang. Mm-vet v2: A challenging benchmark to evaluate large multimodal models for inte-

grated capabilities. *arXiv preprint arXiv:2408.00765*, 2024. 1

[69] Xiang Yue, Yuansheng Ni, Kai Zhang, Tianyu Zheng, Ruoqi Liu, Ge Zhang, Samuel Stevens, Dongfu Jiang, Weiming Ren, Yuxuan Sun, et al. Mmmu: A massive multi-discipline multimodal understanding and reasoning benchmark for expert agi. In *Proceedings of the IEEE/CVF Conference on Computer Vision and Pattern Recognition*, pages 9556–9567, 2024. 8

[70] Mert Yuksekgonul, Federico Bianchi, Pratyusha Kalluri, Dan Jurafsky, and James Zou. When and why vision-language models behave like bags-of-words, and what to do about it? *arXiv preprint arXiv:2210.01936*, 2022. 15

[71] Xiaohua Zhai, Basil Mustafa, Alexander Kolesnikov, and Lucas Beyer. Sigmoid loss for language image pre-training. In *Proceedings of the IEEE/CVF International Conference on Computer Vision*, pages 11975–11986, 2023. 5

[72] Yuexiang Zhai, Hao Bai, Zipeng Lin, Jiayi Pan, Shengbang Tong, Yifei Zhou, Alane Suhr, Saining Xie, Yann LeCun, Yi Ma, et al. Fine-tuning large vision-language models as decision-making agents via reinforcement learning. *arXiv preprint arXiv:2405.10292*, 2024. 8

[73] Jingyi Zhang, Jiaxing Huang, Sheng Jin, and Shijian Lu. Vision-language models for vision tasks: A survey. *IEEE Transactions on Pattern Analysis and Machine Intelligence*, 2024. 1

[74] Pan Zhang, Xiaoyi Dong, Yuhang Zang, Yuhang Cao, Rui Qian, Lin Chen, Qipeng Guo, Haodong Duan, Bin Wang, Linke Ouyang, et al. Internlm-xcomposer-2.5: A versatile large vision language model supporting long-contextual input and output. *arXiv preprint arXiv:2407.03320*, 2024. 13

[75] Deyao Zhu, Jun Chen, Xiaoqian Shen, Xiang Li, and Mohamed Elhoseiny. Minigpt-4: Enhancing vision-language understanding with advanced large language models. *arXiv preprint arXiv:2304.10592*, 2023. 8

[76] Jinguo Zhu, Weiyun Wang, Zhe Chen, Zhaoyang Liu, Shenglong Ye, Lixin Gu, Hao Tian, Yuchen Duan, Weijie Su, Jie Shao, et al. Internvl3: Exploring advanced training and test-time recipes for open-source multimodal models. *arXiv preprint arXiv:2504.10479*, 2025. 2, 13

Appendix

A. ORIC Construction, Analysis, and Evaluation Metrics

A.1. LLM-Guided Sampling Method (Positive Question Construction)

Algorithm 1 Positive Question Construction

Require: Image I, objects $\mathcal{O} = \{(n_i, B_{ij})\}$, integer k
Ensure: Positive question Q

for $i = 1$ to N **do**
  $A_i \leftarrow \text{area}(\bigcup_j B_{ij})$
end for
Sort $\mathcal{O}$ by A_i (descend.)
$\mathcal{O}_{\text{ROI}} \leftarrow$ bottom 50%, $\mathcal{O}_{\text{nonROI}} \leftarrow$ top 50% ▷ Note: Objects exactly at the 50% boundary are classified as non ROI.
$\mathcal{C} \leftarrow \emptyset$
for $o \in \mathcal{O}_{\text{ROI}}$ **do**
  if LLM says "no" for o given $\mathcal{O}_{\text{nonROI}}$ **then**
    $\mathcal{C} \leftarrow \mathcal{C} \cup \{o\}$
  end if
end for
Randomly pick k objects from $\mathcal{C}$ as Q **return** Q

Figure 6 presents the prompt used in LLM-guided rejection sampling for constructing positive questions in the LOPE-3 benchmark. Specifically, {background_objects} serves as a placeholder for all non-ROI objects. For example, if there are three non-ROI objects, they could be represented as ["car", "person", "bottle"]. Meanwhile, {target_object} represents a placeholder for a specific ROI object, such as "vase".

LLM-Guided Rejection Sampling

Given the following background objects: {background_objects}, can you determine the presence of the following target object: {target_object}, with relying on textual priors, common sense knowledge, or general assumptions about object co-occurrences?
Please respond with yes or no.

Figure 6. The prompt for LLM-guided rejection sampling, where {background_objects} acts as a placeholder for all non-ROI objects and {target_object} denotes a placeholder for a specific ROI object.

A.2. CLIP-Guided Sampling Method (Negative Question Construction)

Algorithm 2 Negative Question Construction

Require: Query image I_q, candidate images $\{I_1, \ldots, I_n\}$, non-existent objects $\mathcal{O}_{\text{non}} = \{n_i\}_{i=1}^{M}$, integer k
Ensure: Negative question Q
1: Select the most similar image:

$$I' = \arg\min_{I_i \in \mathcal{I}} \left(1 - \frac{\mathbf{e}_q \cdot \mathbf{e}_i}{\|\mathbf{e}_q\| \|\mathbf{e}_i\|}\right)$$

2: **for** $i = 1$ to M **do**
3: Construct text: $T_i \leftarrow$ "an image contains $\{ n_i\}$"
4: Compute CLIP score: $s_i \leftarrow \text{CLIPScore}(I', T_i)$
5: **end for**
6: Sort $\{n_i\}$ by s_i (descending)
7: Select top k objects: $\mathcal{S} \leftarrow \{n_{i_1}, \ldots, n_{i_k}\}$
8: Construct Q using $\mathcal{S}$ **return** Q

A.3. Evaluation Metric Formulas

For a binary classification problem with labels *yes* and *no*, we define the following terms:

- **TP** (True Positive): Number of samples correctly predicted as *yes* (Ground Truth: *yes*).
- **TN** (True Negative): Number of samples correctly predicted as *no* (Ground Truth: *no*).
- **FP** (False Positive): Number of samples incorrectly predicted as *yes* (Ground Truth: *no*).
- **FN** (False Negative): Number of samples incorrectly predicted as *no* (Ground Truth: *yes*).

The performance metrics include accuracy, the proportion of *yes* predictions, macro precision, recall, and F1 score. These are defined as follows:

Class-wise Metrics:

$$\text{Precision}_{\text{yes}} = \frac{\text{TP}}{\text{TP} + \text{FP}} \tag{6}$$

$$\text{Recall}_{\text{yes}} = \frac{\text{TP}}{\text{TP} + \text{FN}} \tag{7}$$

$$F1_{\text{yes}} = 2 \times \frac{\text{Precision}_{\text{yes}} \times \text{Recall}_{\text{yes}}}{\text{Precision}_{\text{yes}} + \text{Recall}_{\text{yes}}} \tag{8}$$

$$\text{Precision}_{\text{no}} = \frac{\text{TN}}{\text{TN} + \text{FN}} \tag{9}$$

$$\text{Recall}_{\text{no}} = \frac{\text{TN}}{\text{TN} + \text{FP}} \tag{10}$$

$$F1_{\text{no}} = 2 \times \frac{\text{Precision}_{\text{no}} \times \text{Recall}_{\text{no}}}{\text{Precision}_{\text{no}} + \text{Recall}_{\text{no}}} \tag{11}$$

Macro-averaged Metrics:

$$\text{Precision}_{\text{macro}} = \frac{\text{Precision}_{\text{yes}} + \text{Precision}_{\text{no}}}{2} \tag{12}$$

$$\text{Recall}_{\text{macro}} = \frac{\text{Recall}_{\text{yes}} + \text{Recall}_{\text{no}}}{2} = \text{Accuracy} \tag{13}$$

Since our experimental datasets are all balanced, the number of positive and negative samples is equal. In this case, Accuracy = $\text{Recall}_{\text{macro}}$ because accuracy measures the overall proportion of correctly classified samples, and macro recall, being the unweighted average of recall for both classes, reflects the same value.

$$F1_{\text{macro}} = \frac{F1_{\text{yes}} + F1_{\text{no}}}{2} \tag{14}$$

Proportion of Yes Predictions: The proportion of "yes" predictions (i.e., the percentage of all predictions that are classified as "yes") is given by:

$$\text{Yes Proportion} = \frac{\text{TP} + \text{FP}}{\text{TP} + \text{FP} + \text{TN} + \text{FN}} \tag{15}$$

B. Experiment and Analysis

B.1. Evaluated Models

We evaluate **18** widely used LVLMs spanning both encoder-based and encoder-free architectures. The encoder-based models include Qwen2.5-VL-7B-Instruct [4], SmolVLM2-2.2B-Instruct [42], InternVL3-9B [76], Kimi-VL-A3B-Instruct [54], Janus-Pro-7B [9], Llama-3.2-11B-Vision [11], LLaVa-v1.6-7B/13B [39], Phi-3.5-Vision-Instruct [1], Molmo-7B-D-0924 [14], GLM-4V-9B [21], Chameleon-7B [53], VILA-1.5-13B [36], BLIP3 [63], and InternLM-XComposer2.5-7B [74]. Encoder-free models include Fuyu-8B [5], EVE-7B-HD-v1.0 [15], Emu3-Chat [59], and the closed-source GPT-4o-08-06 [26]. What's more, we benchmark against two open-vocabulary detection models: Grounding DINO 1.5 Pro [49] and OWLv2 [44].

B.2. Experimental Prompts

Large Vision-Language Models (LVLMs) Figure 7 illustrates the prompt used for LVLMs in both the POPE and LOPE-3 benchmarks. An example of a specific question is: *"Is there a person in the image?"*.

LVLMs

<image>
Question: {question}
Please answer the question based on the given image.

Figure 7. **The Prompt of LVLMs.** The prompt of a binary classification task for LVLMs is used in all experiments, where {question} serves as a placeholder for a specific query and <image> is the placeholder for a specific image.

We use four distinct prompts in our experiments, detailed below:

- Is there {object} in the image?
- Does the image contain {object}?
- Have you noticed {object} in the image?
- Can you see {object} in the image?

The {object} is the placeholder for a detail object.

Grounding DINO 1.5 Pro Prompt: Figure 8 shows the prompt for Grounding DINO 1.5 Pro. For example, if an image contains four unique objects—sports ball, person, car, and traffic light—the corresponding prompt would be: *"sports ball.person.car.traffic light"*.

Grounding DINO 1.5 Pro

$\{object1\}.\{object_2\}.\cdots.\{object_n\}$

Figure 8. **The Prompt of Grounding DINO 1.5 Pro.** The prompt used for the binary classification task in all experiments with Grounding DINO 1.5 Pro follows a dot-separated notation to specify multiple objects. Placeholders $\{object1\}, \{object_2\}, \cdots \{object_n\}$ represent unique objects in the image, where n denotes the total number of distinct objects.

OWLv2 Prompt: Figure 9 shows the prompt for OWLv2. An example of a specific object is: *"an image of truck"*.

OWLv2

an image of {object}

Figure 9. **The Prompt of OWLv2.** The prompt of a binary classification task for OWLv2 used in all experiments, where {object} serves as a placeholder for a specific object.

Zero-Shot CoT Prompt of LVLMs: Figure 10 shows the zero-shot CoT prompt for LVLMs. An example of a specific question is: *"Is there a person in the image?"*.

Zero-Shot CoT of LVLMs

<image>
Question: {question}
Let's think step-by-step and then answer the question based on the given image.

Figure 10. **The zero-shot CoT Prompt of LVLMs.** The prompt of a binary classification task for LVLMs using zero-shot CoT prompting strategy

B.3. Full Results of Comparison between POPE and ORIC

Table 8 presents a comparative analysis of POPE and ORIC across 19 LVLMs and 2 open-vocabulary detection models. Notably, the macro F1 scores of Llama-3.2-11B-Vision, Chameleon-7B, BLIP-3, and VILA1.5-3B in POPE are comparable to or even exceed those in ORIC. A potential explanation is that these models exhibit a high proportion of "yes" responses in both benchmarks, suggesting a tendency to answer affirmatively regardless of context. This behavior indicates limited object recognition capabilities, as their responses remain consistent across different evaluation settings. Furthermore, the macro precision and recall of other models in ORIC are significantly lower than in POPE, leading to a sharp decline in macro F1 scores. This suggests that ORIC presents a greater challenge for all tested LVLMs, highlighting their struggles with object recognition, particularly when considering contextual incongruity.

B.4. Comparison of Object Size Distribution between POPE, ORIC, and COCO

Figure 11 compares the proportions of small ($< 24 \times 24$ pt^2), medium (24×24–96×96 pt^2), and large ($\geq 96 \times 96$ pt^2) objects in POPE, ORIC, and COCO. In ORIC, small objects are the single largest category at 44.8%—yet they do not constitute a majority: medium objects follow closely at 41.2%, while large objects still make up a substantial 14.0%. Relative to POPE (27.6% small, 34.9% medium, 37.4% large) and COCO (41.3% small, 34.2% medium, 24.4% large), ORIC deliberately boosts the share of small and medium instances at the expense of large ones. This design amplifies the need for fine-grained recognition and scale-robust feature extraction in the face of context incongruity, while still retaining a substantial number of medium and large objects to ensure the benchmark is not solely focused on small instances and can assess model performance across the full spectrum of object scales.

Model	POPE				ORIC			
	Precision	Recall	F1 Score	YP (%)	Precision	Recall	F1 Score	YP (%)
Closed-source								
GPT-4o-2024-08-06	86.84	86.64	86.62	49.39	76.14	75.60	75.45	54.25
Encoder-based								
Llama-3.2-11B-Vision	25.00	50.00	33.33	0.00	25.00	50.00	33.33	0.00
Chameleon-7B	47.08	50.01	33.95	99.29	59.75	50.10	34.08	99.28
BLIP-3	36.20	44.88	37.29	80.30	43.14	49.86	42.99	81.54
VILA1.5-13B	60.87	59.92	57.49	36.80	65.19	62.40	60.41	28.95
GLM-4v-9B	86.55	84.12	83.85	37.30	71.18	64.92	61.99	23.32
Phi-3.5-Vision-Instruct	86.76	86.28	86.23	44.35	68.69	68.06	67.79	40.86
InternLM-XComposer2.5-7B	84.72	83.16	82.98	39.84	73.32	70.35	69.33	33.77
Qwen2.5-VL-7B-Instruct	87.01	84.35	84.06	36.62	75.51	71.67	70.56	30.62
SmolVLM2-2.2B-Instruct	87.57	86.89	86.83	43.56	72.87	71.44	70.95	38.01
Kimi-VL-A3B-Instruct	88.91	87.69	87.59	41.19	74.67	72.28	71.58	34.45
Molmo-7B-D-0924	83.76	81.45	81.03	61.42	78.92	73.74	71.95	69.34
LLaVA-v1.6-Vicuna-13B	88.24	88.14	88.13	51.39	75.29	74.56	74.37	56.94
Janus-Pro-7B	87.32	87.03	87.00	50.65	76.60	75.22	74.83	56.42
InternVL3-9B	88.8	88.69	**88.68**	47.96	77.33	76.95	**76.87**	44.60
Encoder-free								
Fuyu-8B	68.39	53.47	40.48	95.70	44.83	50.16	34.16	99.29
EVE-7B-HD-v1.0	82.19	79.81	79.34	61.36	61.02	56.42	51.59	76.53
Emu3-Chat	87.43	86.72	86.66	43.25	67.74	65.79	64.78	33.41
Open-vocabulary Detection								
OWLv2	86.74	86.55	86.53	53.55	73.02	72.25	72.02	40.85
Grounding DINO 1.5 Pro	85.62	85.05	84.99	56.35	77.02	73.40	72.4	68.30

Table 8. **Full Model Performance Comparison: POPE vs. ORIC.** The table compares POPE and ORIC across various model categories: closed-source, encoder-based, encoder-free, and open-vocabulary detection models. Performance is evaluated using macro precision, recall, and F1 score. The yes proportion (YP (%)) indicates the percentage of "yes" predictions. "Prec." denotes precision, "Rec." denotes recall, and "F1." denotes the F1 score. All values are averaged across four prompts, except for detection models, which use a single prompt without averaging.

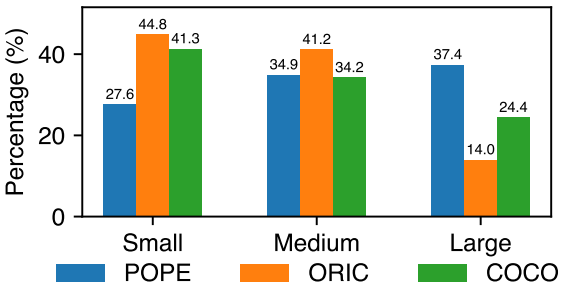

Figure 11. **Object Size Distribution across POPE, ORIC, and COCO.** Percentage distribution of small ($< 24 \times 24$ pt^2), medium (24×24–96×96 pt^2), and large ($\geq 96 \times 96$ pt^2) objects in the POPE, ORIC, and COCO datasets, highlighting ORIC's deliberate shift toward smaller and medium object scales.

C. CLIPScore as a Proxy for Contextual Alignment

While CLIPScore is not a perfect object detector and has known limitations in capturing compositional semantics [29, 70], we use it solely as an external probe to assess the contextual alignment of replaced objects. Specifically, CLIP-guided sampling is applied only to "no"-label cases to select ground-truth nonexistent yet contextually plausible objects with higher CLIPScores, thereby constructing more challenging negatives. Our ablation study 4.2 confirms this strategy by showing a significant reduction in negative recall, indicating increased contextual incongruity.

Importantly, CLIPScore is never used for model evaluation but serves as a heuristic signal of object–context compatibility. To ensure robustness, we validate our findings across three independent CLIP variants in 3.2, all consistently showing that ORIC "yes" or "no" pairs exhibit higher visual similarity than those in POPE, thus increasing task difficulty. While CLIP's co-occurrence bias may contribute

to high scores for out-of-context objects, we argue this reflects its tendency to associate such objects with plausible scenes—precisely the kind of confounding signal our benchmark targets. Despite its limitations, CLIPScore remains a useful proxy for semantic alignment, as supported by recent work [27, 65].

D. Visualization of ORIC Examples

D.1. Error Questions from Human Evaluation

Fig. 12 presents six error cases from **300** sampled questions (150 "yes" and 150 "no" labels) in ORIC using the MSCOCO dataset. We assess two key aspects: accurate object labeling and the appropriateness of visual backgrounds, ensuring incongruous context in both "yes" and "no" questions. The identified errors fall into two categories:

- **Inaccurate Object Labeling**: The presence of objects does not match the actual image content due to errors in human annotation within the MSCOCO dataset.
- **Not Causing the Incongruous Context**: In "yes"-label questions, the visual context aligns with the target object, making the questions less challenging. In "no"-label questions, the visual context does not create incongruity for the nonexistent object.

D.2. ORIC Question Examples

Fig. 13 presents various examples from ORIC. In "yes"-label and "no"-label questions, visual contexts are incongruous with the question-related objects. Our LLM-guided and CLIP-guided sampling method effectively generates challenging questions considering contextual incongruity.

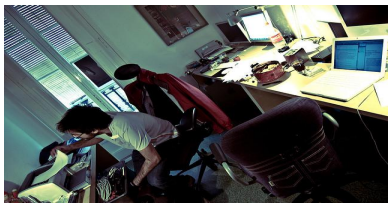

POPE: Is there a mouse in the image?
Label : No
Inaccurate Object Labeling: The keyboard is present while labeling errors.

Question: Is there a mouse in the image?
Label: Yes
Not Causing The Incongruous Context: The office area provides a congruous context for a mouse.

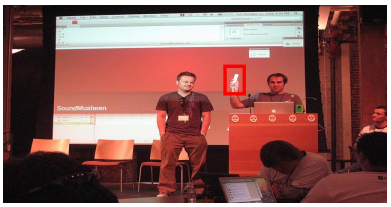

Question: Is there a remote in the image?
Label: Yes
Not Causing The Incongruous Context: The conference room provides a congruous context for a remote.

Question: Is there a bed in the image?
Label: No
Not Causing The Incongruous Context: The living room doesn't provide an incongruous context for a nonexistent bed.

Question: Is there an orange in the image?
Label: No
Not Causing The Incongruous Context: The tennis court doesn't provide an incongruous context for a nonexistent orange .

Question: Is there a skateboard in the image?
Label: Yes
Not Causing The Incongruous Context: The skatepark doesn't provide an incongruous context for a nonexistent skateboard.

Figure 12. **Error Examples of ORIC from Human Evaluation.** There are six error cases among the **300** sampled questions in ORIC using the MSCOCO dataset, resulting in an error rate of 2%. These errors can be classified into two categories. **Inaccurate Object Labeling** occurs when the labeled object's presence does not match the actual content of the image. **Not Causing the Incongruous Background** includes cases where the visual context aligns with an existent object in a "yes"-label question or does not introduce incongruity for a nonexistent object in a "no"-label question.

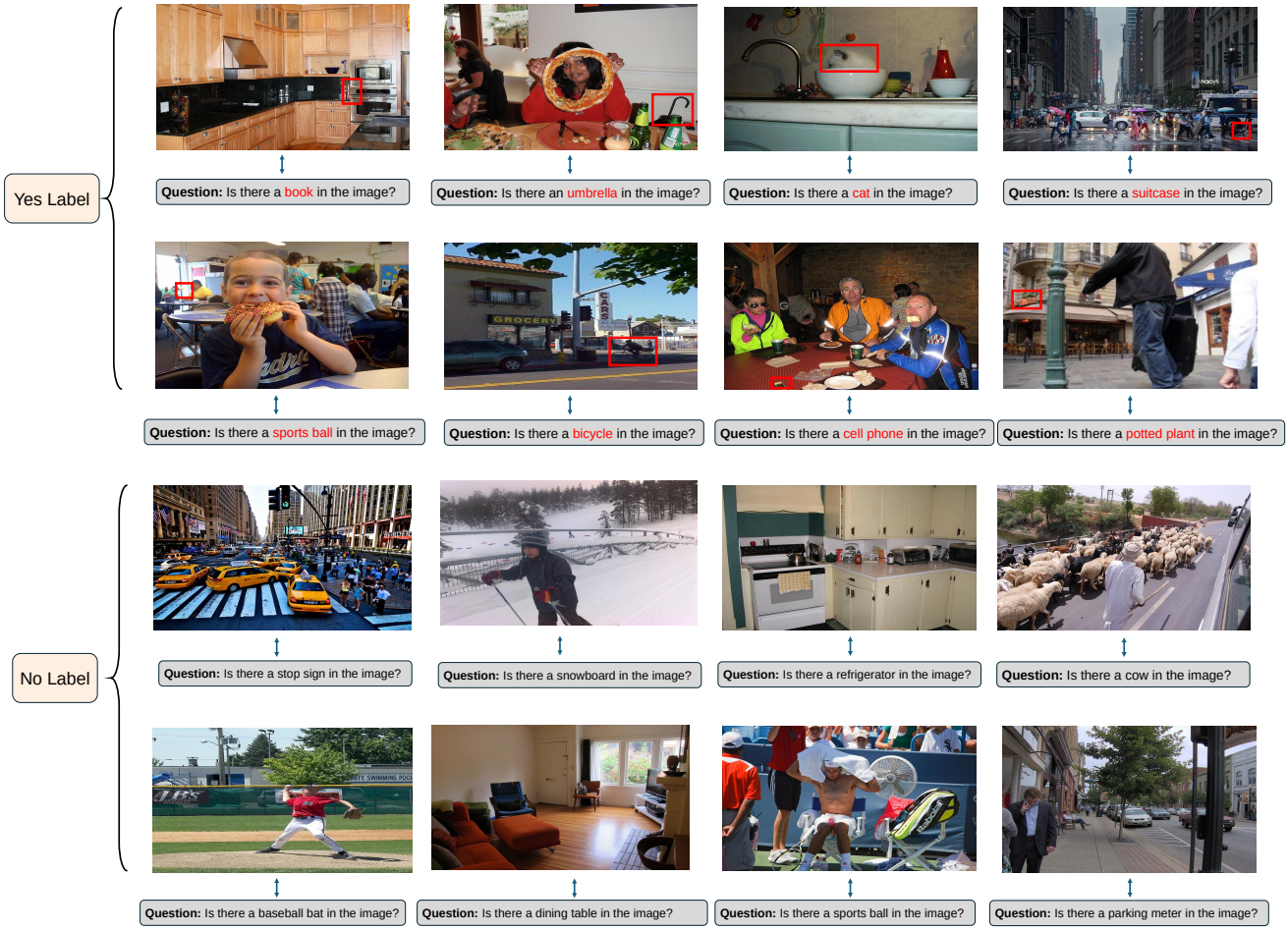

Figure 13. **Question Examples of ORIC.** The figure shows sampled question examples from ORIC using the MSCOCO dataset. The first and second rows contain questions labeled "yes," while the third and fourth rows contain questions labeled "no." The red box highlights the bounding boxes of existing objects in "yes"-label questions.